Biochimica et Biophysica Acta, 1153 (1993) 191–202

BBAMEM 76141

Membrane orientation of transmembrane segments 11 and 12 of MDR- and non-MDR-associated P-glycoproteins

Jian-Ting Zhang[1] and Victor Ling *

Division of Molecular and Structural Biology, Ontario Cancer Institute, Department of Medical Biophysics, University of Toronto, 500 Sherbourne Street, Toronto, M4X 1K9 (Canada)

(Received 10 March 1993)
(Revised manuscript received 21 July 1993)

Key words: MDR; Multidrug resistance; Drug resistance; Mutagenesis; Topology; Membrane orientation; P-glycoprotein

P-glycoprotein (Pgp) is a polytopic plasma membrane protein thought to function as a drug efflux pump. Two functional groups of Pgp have been identified in mammalian cells. One group (classes I and II) is associated with MDR and the other (class III) is not. Transmembrane (TM) sequences in Pgp have been postulated to be important for determining drug specificity. TM11 and TM12 have been predicted to bind drugs and play an important role in determining drug specificity of MDR-associated Pgps. Whether or not the membrane insertion and orientation of these TM segments differ amongst the different classes of Pgp has not been examined directly. In this study, we showed that membrane insertion and orientation of TM11 and TM12 of the MDR-associated Pgp may differ from the non-MDR-associated Pgp using an in vitro transcription and translation system. Charged amino acids surrounding TM domains are thought to be important in determining the topology of membrane proteins. The positively charged amino acids surrounding TM11 and TM12 of these two forms of Pgp are different. By site-directed mutagenesis we showed that these amino acids may affect the membrane orientation but not membrane insertion of these TMs. These results raise the possibility that a difference in membrane anchorage may be a underlying cause for the functional difference between the two groups of Pgp.

Introduction

P-glycoprotein (Pgp), the product of multidrug resistance (*mdr*) genes in mammals, is predicted to be a polytopic membrane glycoprotein. It belongs to a superfamily of transmembranes which include the cystic fibrosis transport regulator, bacterial hemolysin B, *S. cerevisiae* STE6, and peptide transporter associated with class I MHC antigen presentation [1–4]. Pgp probably functions as a drug efflux pump in tumor cells [5]. There are three classes of structurally related Pgp in rodents and two in human [5]. Classes I and II Pgp are able to confer an MDR phenotype when transfected in mammalian cells of different species [5–7]; however, cells transfected with the class III Pgp do not confer a drug resistance phenotype [6,8].

The hydrophobic domains of Pgp have been suggested to be important for the MDR function of Pgp [9]. Replacement of the hydrophobic domains of class I Pgp with those of class III Pgp destroyed the MDR function of the class I Pgp. Exchange of either the N-terminal or the C-terminal ATP-binding domains did not alter the MDR function [9]. Recently, Gros et al. [10] demonstrated that a single amino acid substitution (serine 941 to phenylalanine) within the predicted TM11 of class I and class II (position 939) dramatically altered the overall degree of drug resistance conferred by class I and II Pgp. A domain which binds photoactive drugs has been mapped in close proximity to the putative TM11 and TM12 [11], and has now been defined within TM11 (Georges and Ling, unpublished observation). These studies indicate that the predicted TM segments with their surrounding sequences play an important role in determining the MDR function of Pgp.

It has been suggested previously that TM segments in a polytopic membrane protein integrate into membranes by a series of alternating signal and stop-trans-

* Corresponding author. Fax: +1 (416) 9266529.
[1] Current address: Department of Physiology and Biophysics, University of Texas Medical Branch, Galveston, TX 77555-0641, USA.
Abbreviations: Pgp, P-glycoprotein; MDR, multidrug resistance; TM, transmembrane; ABC, ATP-binding cassette; SRP, signal recognition particle; SDS-PAGE, sodium dodecyl sulfate-polyacrylamide gel electrophoresis; RM, rough microsomes; KRM, high salt-treated rough microsomes; NEM, *N*-ethylmaleimide-treated rough microsomes. PNGaseF, peptide *N*-glycosidase F; RNasin, RNAase inhibitor; kb, kilobase(s); kDa, kilodalton(s).

fer sequences [12]. It has also been suggested that study of truncated constructs containing two consecutive TM domains of a polytopic membrane protein may reflect the natural alternating signal and stop-transfer functions of TM segments in a polytopic membrane protein [13]. In this study, we investigated membrane association differences between the truncated Pgp isoforms containing TM11 and TM12. The role of the amino acids surrounding TM11 and TM12 on membrane integration and orientation was investigated. Our approach takes advantage of the experimental convenience of the in vitro transcription and cell free translation/translocation system. Previously, this system had been used successfully to investigate the topological structure and membrane insertion of small domains in polytopic membrane proteins [13,14] and the full-length mouse *mdr1* Pgp [15]. Our results show that the truncated MDR-associated Pgps (class I and II) may have characteristics of membrane association and orientation different from the non-MDR-associated Pgps (class III), and that positive charges may be important in determining their orientation, but not membrane targeting and insertion.

Materials and Methods

Materials

pGEM-4z plasmid, SP6 and T7 RNA polymerase, RNasin, ribonucleotides, RQ1 DNase, rabbit reticulocyte lysate, wheat germ extract and dog pancreatic microsome membranes were obtained from Promega. [^{35}S]Methionine and Amplify for fluorography were purchased from Amersham. m^{7}G(5′)ppp(5′)G cap analog was obtained from Pharmacia LKB. Peptide *N*-glycosidase F, T4 DNA ligase, Klenow polymerase and restriction endonucleases were obtained from Boehringer Mannheim. M13mp19 was purchased from Bethesda Research Laboratories. Polynucleotide kinase was from New England Biolabs. All other chemicals were obtained from Sigma or Fisher Scientific.

Construction of cDNA fragments in an expression vector

The cDNA fragments were released from their full-length or original clones [15,16] separated on and purified from low melting point agarose gel and subsequently subcloned into pGEM-4z. These constructs are shown in Fig. 1b. The SP6 promoter is used to initiate

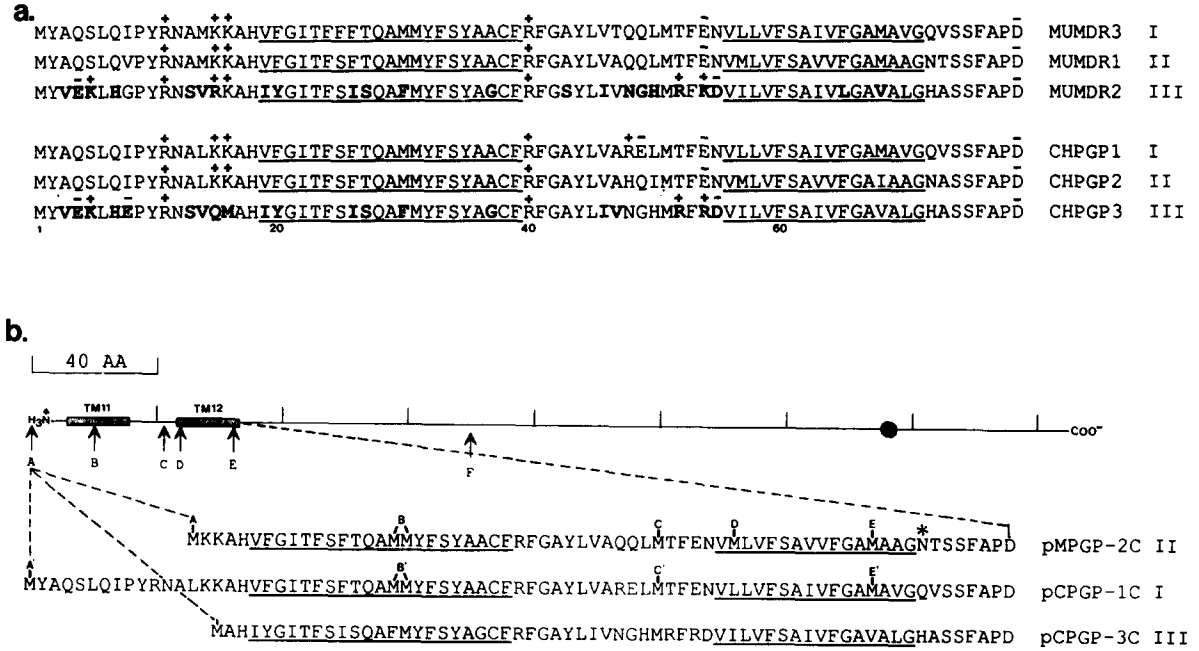

Fig. 1. (a) Sequence comparison between the three classes of P-glycoprotein from mouse (MU) and Chinese hamster (CH). In each species, class I, II and III Pgps are indicated. The putative TM11 and TM12 are underlined and the charged amino acid residues are indicated by (+) and (−). The amino acid residues that are conserved between class I and II, but different in class III Pgp are in bold. (b) Outline of the truncated P-glycoprotein molecules and the amino acid sequences surrounding TM11 and TM12 of all three classes. Arrows indicate the potential in-frame ATG initiation sites. The stippled bars are predicted TM segments. The solid circle is the monoclonal antibody C219 epitope. The amino acid sequences of TM segments and their surrounding regions encoded by all three truncated cDNA constructs are shown. They all share a similar C-terminal-coding domain, but different starting point for translation. Class I and III are from Chinese hamster and class II is from mouse. The potential glycosylation site is indicated by (*). The N-terminal methionine (M) coded by potential initiator ATG's are indicated by A, B, C, D and E for class II and A′, B′, C′ and E′ for class I Pgp.

transcription of sense RNA's. All the constructs encode the two putative TM domains (TM11 and TM12) at the N-terminus and a long C-terminal hydrophilic domain with an ATP-binding site. Their in-frame ATG's are used as translation initiation sites (see Fig. 1). The resulting clones were named pCPGP-1C (Chinese hamster pgp1, class I), pMPGP-2C (mouse *mdr1*, class II) and pCPGP-3C (Chinese hamster *pgp3*, class III). All constructs were confirmed by double-strand DNA sequencing.

Site-directed mutagenesis of the truncated class II P-glycoprotein

A 500 bp cDNA fragment of the mouse *mdr1* cDNA was released from pMPGP-2C by double digestion with *Eco*RI and *Pst*I, purified on a low melting point agarose gel, and subcloned into the *Eco*RI and *Pst*I site of M13mp19. The M13 DNA was propagated for three cycles in bacterial strain BW313 before the U-containing single strand DNA was prepared for synthesis of the mutagenic strand. The mutant DNA was screened by either filter lifting using an end-labelled oligonucleotide as probe or restriction mapping of mutation-introduced restriction site. All mutations in DNA were confirmed by sequencing. Once a mutation was identified, double-strand M13 DNA was prepared by standard procedures. The mutated *mdr1* cDNA fragment was released and purified from M13 DNA by *Eco*RI and *Pst*I digestion and cloned back into the pMPGP-2C DNA. The oligonucleotides used to produce mutations in the mouse *mdr1* cDNA were: 5'-CTCATGAGGTTTAAAAATGTTATG-3' (M1); and 5'-GCGATGAATCAAGCACACGTG-3' (M2). M1 was used to change threonine-52 and glutamate-54 to arginine and lysine residues, respectively. M2 was used to change lysine-15 and 16 to asparagine and glutamine residues, respectively. The oligonucleotide used to produce a mutation in the Chinese hamster *pgp1* cDNA was 5'-GAAAATATGTATAACCAGAGC-3'. This mutation introduced a potential N-linked glycosylation site at amino acid residue-3. All oligonucleotides were purified by gel electrophoresis and were 5' phosphorylated using T4 polynucleotide kinase.

In vitro transcription and translation

About 6 μg of plasmid DNA linearized with different restriction enzymes was transcribed with SP6 (sense strand) or T7 (antisense strand) RNA polymerase in the presence of 5 A_{260} Units/ml cap analog $m^7G(5')ppp(5')G$ as described previously [17]. Removing DNA templates with RQ1 DNase after transcription, and purification of RNA transcripts were carried out according to the protocols supplied by Promega. The RNA from each transcription was dissolved in 14 μl diethyl pyrocarbonate-treated water containing 1 Unit/μl RNasin, a ribonuclease inhibitor. The yield of RNA was usually around 10 μg per reaction and homogenous in size as analyzed by using agarose gel electrophoresis and autoradiography of transcripts generated in the presence of alpha-[^{32}P]-UTP. There is no premature termination of transcription in these reactions.

Translation and translocation in rabbit reticulocyte lysate and wheat germ extracts were performed as suggested by the supplier (Promega). Proteinase protection and separation of membrane-associated proteins from non-membrane proteins after Na_2CO_3 (pH 11.5) extraction were performed as described previously [18]. PNGaseF (a peptide endoglycosidase) treatment was done as described by Zhang and Ling [15]. Since detergents were included in the reaction, the luminal peptides and sugars were presumably exposed to the PNGaseF. For PNGaseF treatment of membrane-protected fragments of proteolysis, the proteinase digestion was stopped by adding phenylmethylsulfonyl fluoride (PMSF) to a final concentration of 10 mM. The membrane fraction was then microfuged for 15 min and the membrane pellet was washed with STBS (0.25 M sucrose, 10 mM Tris-HCl (pH 7.5), 150 mM NaCl) containing 10 mM PMSF, and microfuged again for 15min. Finally, it was solubilized for PNGaseF treatment. Preparation of SRP-depleted microsomal membranes (K-RM) by 0.5 M potassium acetate washing was performed as described earlier [19]. The removal of docking protein activity of RM by 2 mM *N*-ethylmaleimide (NEM) alkylation or by trypsin digestion were performed as described by Gilmore et al. [20] and Meyer and Dobberstein [21] respectively. For fluorographic analysis, [^{35}S]-methionine was added to all reactions to a final concentration of 1 μCi/μl. Immunoprecipitation of the translation products using monoclonal antibody C219 was performed as described before [22].

Microsequencing of radiolabelled peptides

Translation was carried out in the presence of [^{35}S]methionine (1 μCi/μl) and [^{3}H]phenylalanine (5 μCi/μl). About 10 μl reaction was separated by SDS-PAGE and transferred onto a PVDF membrane according to Moos et al. [23]. After transfer, the PVDF membrane was rinsed with water, air dried and exposed to X-ray film for 1 day. The PVDF membrane slices corresponding to each peptide were excised and used for amino acid sequencing on a Porton model 2090E gas phase sequencer. Fractions from each cycle was collected and subjected to scintillation counting. Incorporated radioactivity associated with each cycle was obtained by subtracting background using a precycle as control. Incorporated radioactivity for [^{35}S] methionine and for [^{3}H]phenylalanine was determined in appropriate channels on a Beckman LS6000SC scintillation counter. Scintillation counting efficiency was

corrected using added internal standards. Overlap of the ^{35}S signal into the ^{3}H channel was corrected in each sample. There was no overlap of the ^{3}H signal into the ^{35}S channel.

SDS-PAGE analysis

SDS-PAGE, Amplify treatment and film exposure were performed as described previously [15]. Molecular weight markers used were from Bethesda Research Laboratory. For quantitation, each band was cut out of the gel and scintillation counted or the intensity of each band was determined by scanning the film using a densitometer (Molecular Dynamics).

Results

Alignment of the amino acid sequence surrounding TM11 and TM12 of all three classes of rodent Pgps is shown in Fig. 1a. The predicted extracellular loop formed between these two TM segments has higher net positive charges in class III than in class I and II Pgp. Fig. 1b shows the outline of the truncated class I (Chinese hamster *pgp1*), class II (mouse *mdr1*) and class III (Chinese hamster *pgp3*) Pgp molecules and amino acid sequences surrounding TM11-TM12. These truncated proteins contain two predicted TM segments (TM11 and TM12) and an extensive hydrophilic domain of 289 amino acids with an ATP-binding site and an epitope for monoclonal antibody C219 (indicated by a solid circle). The cDNA constructs that encode these truncated Pgps were designed so that an internal ATG immediately upstream of TM11 can be used as a translation initiation site.

In vitro translation of the truncated class II P-glycoprotein molecule

In vitro translation of the pMPGP-2C RNA transcript in a rabbit reticulocyte lysate produced six peptides of M_r 36000, M_r 34000, M_r 32000, M_r 31000, M_r 30000 and M_r 19000 respectively (labeled as A, B, C, D, E and F in lane 3, Fig. 2a). These six peptides correspond in size to products initiated at the six available predicted in-frame ATGs of the transcript (see Fig. 1b). All the peptides can be immunoprecipitated with C219, confirming that they all have the correct reading frame and an intact C-terminal end of the protein (data not shown, but see lane 2, Fig. 2b). No translation products were observed when the mRNA transcripts were excluded from the translation reaction (lanes 1 and 2, Fig. 2a). To confirm that the translated peptides were indeed due to initiations at the predicted ATG's, we performed microsequencing of the major peptides radiolabeled with [^{35}S]methionine and [^{3}H]phenylalanine (see Materials and Methods). The results are shown in Fig. 3. A strong [^{35}S] methionine signal was observed in the first cycle of Edman degradation in all the peptides analyzed (see Fig. 3a, 3b, 3e and 3f), confirming that these peptides result from initiations at internal ATG's and not due to unsuspected degradations. Peptide C also has a significant [^{35}S]methionine signal at cycle 7, corresponding to the expected methionine residue at that position (Fig. 3e). The [^{3}H]phenylalanine signal was also observed at cycle 7 (Fig. 3c) and cycle 3 (Fig. 3d) for peptides A and B respectively, consistent with the expected position of the phenylalanine residue in these peptides. The incorporation of [^{3}H]phenylalanine into peptide C was too low to obtain meaningful results. However, as noted above, the presence of the [^{35}S]methionine signal at cycle 7 of peptide C confirmed its sequence. These microsequencing results and the monoclonal antibody C219 binding studies (see results in Fig. 2b) are completely consistent with our conclusion that peptides A–E are generated from predicted internal ATG's.

When RM was included in the translation, only five peptides were observed (lane 4, Fig. 2a). While the intensity of peptides-B, C and D was decreased, a new band with M_r 33000 (indicated by C^g) was generated and the intensity of the peptide E was increased (lane 4). Therefore, it is likely that the peptide C^g is the translocated and post-translationally processed (by signal sequence cleavage possibly at Ala-70 or Gly-71 in Fig. 1, and N-linked glycosylation) products of peptides B and C. Although we can not rule out the possibility that the peptide C^g is also generated from the peptide A, the same intensity of peptide A observed in the presence and absence of RM makes it unlikely. Differential centrifugation of the products translated in the presence of RM indicates that the majority of the peptide A and peptide C^g remained in the membrane fraction while most of peptide B and F were in the non-membrane fraction (lanes 5 and 6, Fig. 2a). The M_r 30000 peptide E produced in the presence of RM apparently consists of two components (indicated by single and double arrow head respectively in Fig. 2a). The component indicated by a single arrow head (Fig. 2a) was in the non-membrane fraction (lane 6). It is presumably peptide E, which does not have putative TM segments. The component denoted by a double arrow head has a slightly smaller size than the peptide indicated by a single arrow head and is RM vesicle-associated (lane 5, Fig. 2a). Upon Na_2CO_3 (pH 11.5) treatment which releases content and peripheral proteins from RM vesicles [18], peptide C^g was released to the non-membrane fraction, whereas about 50% of peptide A remained with the membrane pellet. This result suggests that peptide A is integrated into RM membranes and that peptide C^g may be a content peptide inside RM vesicles. The observation of peptide A in supernatant fraction after alkaline treatment is probably because the alkaline extraction was not per-

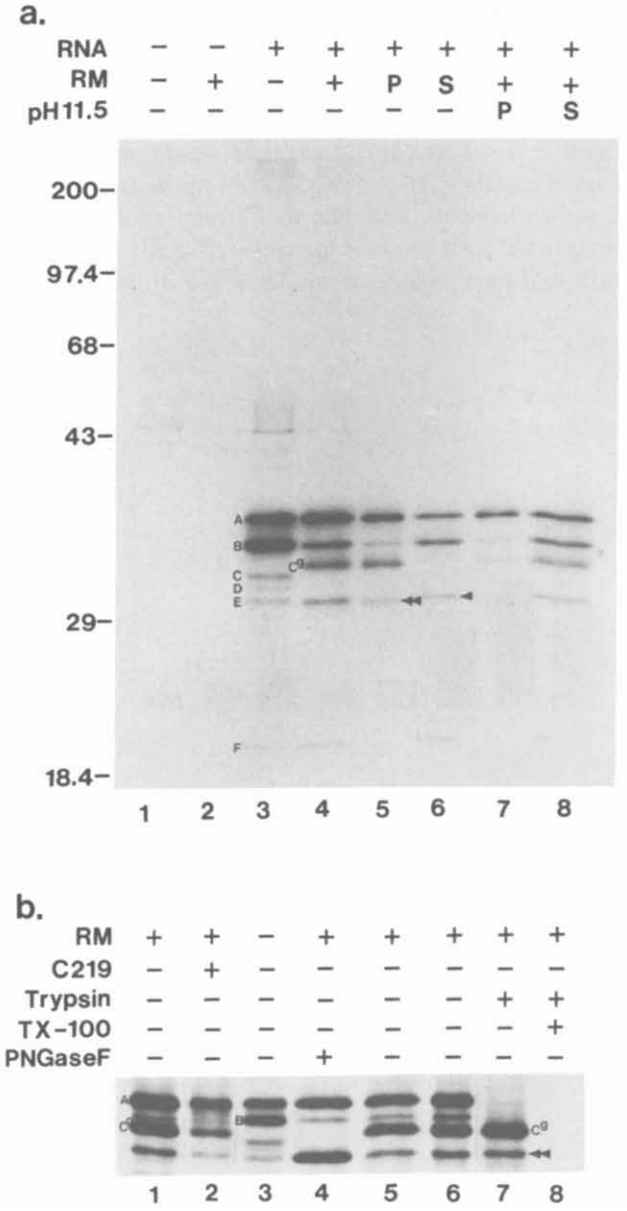

Fig. 2. (a) Translation of the truncated class II (mouse) Pgp DNA (pMPGP-2C). In vitro transcript of the pMPGP-2C DNA was used to direct translation in a rabbit reticulocyte lysate system. Five peptides produced in the absence of RM were labelled as A, B, C, D and E, respectively (lane 3). A new band generated in the presence of RM (lane 4) was indicated by C^g. The intensity of peptide E in the presence of RM is higher than that in the absence of RM (compare lanes 3 and 4) and this increase is caused by a generation of another peptide (indicated by double arrowhead) in the presence of RM. The peptide (indicated by double arrowhead) is membrane associated while the peptide E (indicated by single arrow head) is soluble (lanes 5 and 6). Molecular mass markers (Bethesda Research Lab.) shown on the left are in kilodaltons. P = pellet; S = supernatant. (b) Post-translational treatment of the membrane-associated translation peptides of pMPGP-2C. Translation of pMPGP-2C was carried out in the presence of RM and the membrane fraction was subsequently analyzed directly on SDS-PAGE (lane 1), immunoprecipitated with C219 (lane 2), treated with endoglycosidase PNGaseF (lane 4), or treated with trypsin in the absence (lane 7) or presence (lane 8) of 1% Triton X-100. Lanes 5 and 6 are control reactions for PNGaseF (lane 4) and trypsin (lane 7) treatment respectively. No product was precipitated with normal mouse IgG molecules (data not shown).

formed on RMs which have been previously sedimented to remove free peptides (i.e. not associated with membranes). The peptide indicated by a double arrowhead is also sensitive to Na_2CO_3 extraction (lane 8, Fig. 2a), suggesting that it is not integrated into membranes. Possibly, it is the non-glycosylated form of peptide C^g (see below in Fig. 2b).

Membrane orientation of the M_r 36000 peptide A and M_r 33000 peptide C^g of the truncated class II P-glycoprotein

To study the membrane orientation of the M_r 36000 peptide A which contains both TM segments and the long C-terminal hydrophilic domain of 289 amino acid residues, trypsin treatment of the membrane-associated translation product was first analyzed. If the long C-terminal end is located in the lumen of RM by anchorage in the membrane through the two TM segments, peptide A will be protected from trypsin digestion by RM membranes (see Fig. 4, model II). On the other hand, it will be sensitive to trypsin if the long C-terminal end is outside of RM vesicles (see Fig. 4, model I). As shown in Fig. 2b, peptide A was sensitive, whereas peptide C^g and the peptide indicated by a double arrow head were resistant to trypsin treatment (lane 7). This suggests that peptide A has its long C-terminal hydrophilic domain located on the outside of RM, consistent with the results of both in vitro and in vivo studies of full length Pgp [4,15]. It also suggests that peptide C^g and the peptide indicated by a double arrow head are located in the lumen of RM (see Fig. 4, model II). Both trypsin-resistant peptides can still be immunoprecipitated with monoclonal antibody C219, suggesting that their C-terminal C219 epitope is still intact (data not shown). An Arg residue (see Fig. 1) present in the loop linking TM11 and TM12 of class II Pgp is a possible trypsin cleavage site for generating a fragment with a similar size of C^g. However, this possibility is unlikely because the Arg-40 residue (as numbered in Fig. 1a) is located at the very end of the TM11 of MUMDR1 (Fig. 1a). It is too close to the membrane to be accessible to trypsin digestion. Therefore, the possibility that the peptide C^g is a degradation product of the peptide A can be ruled out.

Peptide A has a potential N-linked glycosylation site at amino acid residue-72 (see Fig. 1a) on the C-terminal side of TM12. If the C-terminal domain with the residue-72 of TM12 is located inside RM lumen, peptide A will probably, although not necessarily, be glycosylated. However, the peptide A-assocated with RM is not glycosylated. The apparent size of the translated peptide A is not changed by including RM (compare lanes 1 and 2 of Fig. 2a) nor by PNGaseF treatment (compare lanes 3 and 4 of Fig. 2a), which cleaves between the innermost residue of the oligosaccharide chain and the asparagine residue (compare lanes 4 and

5 in Fig. 2b). Therefore, these results are consistent with the conclusion that the C-terminal end of peptide A is located on the outside of RM (model I in Fig. 4). The trypsin resistant peptide C^g (lane 7 in Fig. 2b) can be changed to a 30 kDa peptide (double arrow head) by PNGaseF treatment. This observation further rules out the possibility that peptide C^g is a trypsin degradation product of peptide A since peptide A is not modified by N-linked glycosylations whereas the peptide C^g is. We have also performed an experiment of double treatment with trypsin and PNGaseF on membrane fractions of a translation and have shown that all the trypsin resistant peptides at the size of C^g is sensitive to PNGaseF treatment (data not shown). Taken together, the above results show that peptide A-associated with RM has its C-terminal end located outside of RM whereas peptide C^g and the peptide indicated by a double arrow head are in the lumen of

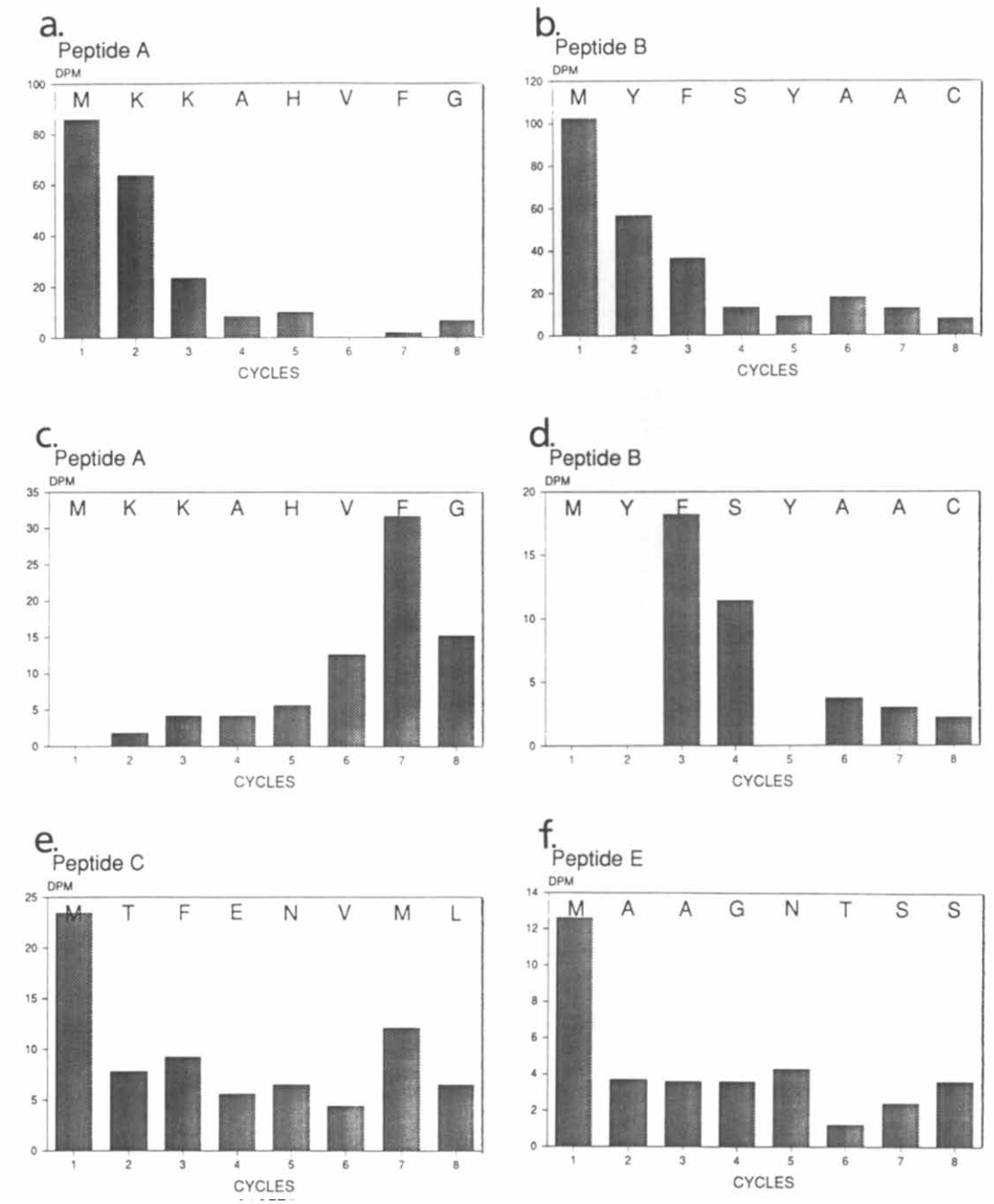

Fig. 3. Microsequencing of in vitro labelled peptides. [^{35}S]Methionine and [^{3}H]phenylalanine labelled peptides were separated, isolated on SDS-PAGE and subjected to radiomicrosequencing. Incorporated radioactivity of [^{35}S]methionine for each cycle of Edman degradation for peptide A (panel a), peptide B (panel b), peptide C (panel e), and peptide E (panel f) was compared with the predicted sequences of these peptides. Similarly, incorporated radioactivity of [^{3}H]phenylalanine for peptides A (panel c) and B (panel d) is shown. Errors associated with scintillation counting is estimated to be 8% or less.

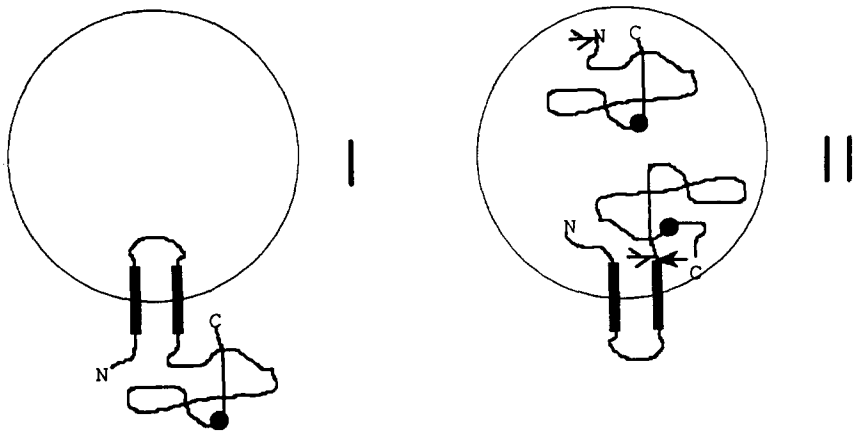

Fig. 4. Schematic diagram of possible orientations of nascent peptide A. In model I, the long C-terminal end of peptide A is on the outside of RM vesicles (cytoplasmic) and therefore is accessible to proteinase digestion. In model II, peptide A has the C-terminal end located in the lumen of RM vesicles (extracellular) and is proteinase resistant. The peptide shown in the lumen of RM in model II is peptide C^g, which is resistant to proteinase digestion but sensitive to alkaline extraction. The solid circle represents the monoclonal antibody C219 epitope. The bold bars indicate the putative transmembrane segments. Oligosaccharide chains are indicated by branched structure. The arrow in model II shows a potential signal sequence cleavage site. Once it is cleaved, the internal portion will be released into the RM lumen and the TM segments will remain associated with membrane.

RM. The orientation of peptide A is consistent with the predicted topology of native Pgp based on hydropathy analysis [24].

The truncated class I Pgp molecule integrates into membranes efficiently and has a similar membrane orientation as class II Pgp

We next examined the membrane integration and orientation of the truncated Chinese hamster *pgp1* Pgp (class I) using the same strategy as that used to study the truncated class II Pgp (see above). As shown in Fig. 5, four peptides of M_r 36000, M_r 33000, M_r 32000 and M_r 31000 (labelled as A′, B′, C′ and E′) were produced from the four in-frame ATG initiation sites of pCPGP-1C RNA (lane 1, also see Fig. 1b for primary sequence). A peptide corresponding to peptide D of truncated class II Pgp is not observed here because the corresponding ATG initiator is not present. In the presence of RM, the intensity of peptides B′ and C′ is decreased and a new peptide of 29.5 kDa (indicated by double arrow head) is observed (lane 2, Fig. 5). This peptide is the translocated and post-translationally processed form of peptides B′ and C′. Truncated class I Pgp does not have a potential N-linked glycosylation site, therefore, no glycosylated peptide equivalent to C^g of class II Pgp was observed. As discussed above for the origin of the peptide C^g of class II Pgp, it is unlikely that the peptide of 29.5 kDa is generated from the peptide A′ because the intensity of the peptide A was not decreased in the presence of RM.

The majority of peptide A′ and the M_r 29500 peptide (indicated by double arrow head) remained in the membrane pellet while more than 50% of the other peptides were in the non-membrane fraction (lanes 3 and 4, Fig. 5). However, extraction with 0.1 M Na_2CO_3 (pH 11.5) released the M_r 29500 peptide (double arrow head) to the supernatant fraction while most of peptide A′ still remained with the pellet (lanes 5 and 6, Fig. 5). Therefore, peptide A′ was anchored in the membrane and the M_r 29500 peptide was in the RM lumen. After proteinase K digestion of the membrane fraction, peptide A′ disappeared whereas the M_r 29500

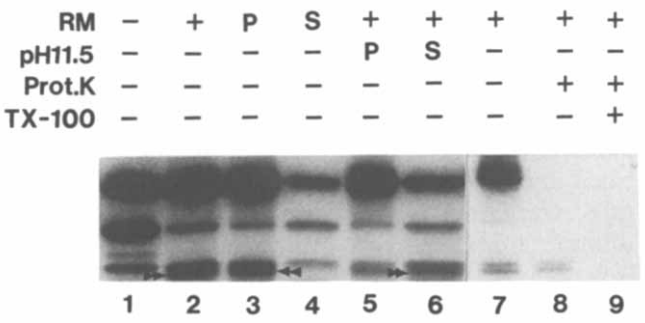

Fig. 5. In vitro translation of pCPGP-1C transcripts and post-translational treatment of the peptide products. In vitro transcripts of the pCPGP-1C DNA were used to direct translation in a rabbit reticulocyte lysate. Four peptides of M_r 36000, M_r 33000, M_r 32000 and M_r 30000 produced in the absence of RM were labeled as A′, B′, C′ and E′, respectively (lane 1). In the presence of RM, a new peptide (indicated by double arrow head) with a molecular weight smaller than the peptide E′ is produced (lane 2). While the majority of peptide A′ and the M_r 30000 peptide (double arrow head) is associated with membrane (lane 3), the peptide E′ and > 50% of peptide B′ were in the supernatant fraction (lane 4). However, the alkaline extraction released the M_r 29500 peptide (double arrow head) to supernatant fraction whereas the peptide A′ remains with the membrane fraction (lanes 5 and 6). The peptides A′ and B′ are sensitive to proteinase K treatment while the M_r 29500 peptide (double arrow head) is resistant (lane 8). The M_r 29500 peptide became proteinase sensitive when 1% Triton X-100 was included in the digestion (lane 9). Lane 7 is an untreated control for proteinase digestion in lane 8.

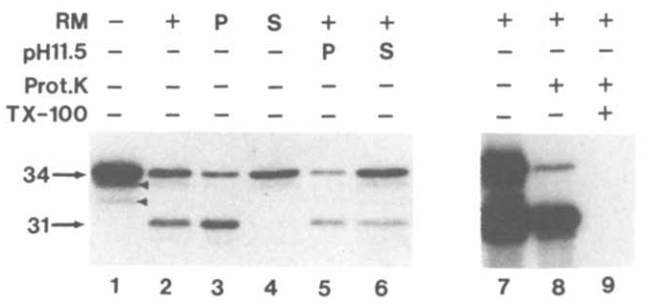

Fig. 6. In vitro translation of the truncated pCPGP-3C DNA transcripts. DNA encoding the truncated class III Pgp was constructed (see Fig. 1) and used to direct in vitro translation in a rabbit reticulocyte lysate. A major product of M_r 34000 with two minor band (indicated by arrow heads) were generated in the absence of RM (lane 1) and an additional band of M_r 31000 was generated when RM was included in the translation (lane 2). The majority of M_r 34000 peptides is not membrane-associated (lanes 4 and 6). The M_r 31000 peptide is membrane-associated (lane 3), sensitive to alkaline extraction (lane 6) and resistant to proteinase K digestion (lane 8), suggesting that it is in the lumen of RM. About 5% of the M_r 34000 peptide is also resistant to proteinase K digestion (lane 8). Lane 7 is an untreated control reaction for the proteinase digestion of lane 8. The gel for lanes 7–9 was exposed for longer time than other lanes to show clearly the proteinase resistant fraction of the M_r 34000 peptide.

peptide was resistant to digestion (lane 8, Fig. 5). The above results suggest that the ATP-binding domain of peptide A′ is located on the outside of the RM and confirms that the M_r 29500 peptide (double arrow head) is in the RM lumen (see Fig. 4). It is not known why some of the M_r 31000 peptide (E′) was also resistant to proteinase K digestion (lane 8, Fig. 5). One possible explanation is that some of the M_r 31000 peptides generated in the presence of RM are translocated and processed products like the M_r 29500 peptide except that the signal sequence cleavage site is different from that of the processed M_r 29500 peptide.

Membrane integration and orientation of the truncated class III P-glycoprotein

We next examined the membrane integration and orientation of the corresponding truncated non-MDR-associated class III Pgp (Chinese hamster *pgp3*, pCPGP-3C DNA, see Fig. 1b). As shown in Fig. 6, one major peptide of M_r 34000 was produced in a rabbit reticulocyte lysate. Two smaller products (indicated by arrows in Fig. 6) are probably translation products initiated from in-frame ATG's downstream. Less efficient translation initiation at the downstream ATG's of class III Pgp is probably due to the lack of Kozak consensus sequences for the initiation of translation. This is consistent with the low translation efficiency of peptide D of class II Pgp which also does not have the Kozak consensus sequence for initiation (see Fig. 2a). The intensity of the M_r 34000 peptide was reduced and another peptide of M_r 31000 was generated when RM was included in the translation. Differential centrifugation indicated that most (~70%) of the M_r 34000 peptide was not associated with membrane while the M_r 31000 peptide remained with the membrane pellet (lanes 3 and 4, Fig. 6). The sensitivity of the M_r 31000 peptide to 0.1 M Na_2CO_3 (pH 11.5) extraction suggests that it is not anchored in the membrane (lanes 5 and 6, Fig. 6).

Proteinase K treatment of the membrane-associated translation product of pCPGP-3C suggests that a small fraction (~5%) of the membrane-associated M_r 34000 peptide is resistant to digestion (lane 8, Fig. 6). This indicates that some of the membrane-associated M_r 34000 peptide product of pCPGP-3C has its long C-terminal end located inside the RM lumen. The loop between the two TM segments of the inverted molecules is presumably too small to be digested by proteinases. Therefore, no size shift of this proteinase resistant band was observed. The M_r 31000 peptide appears to be protected from proteolysis, confirming that it has been translocated into the RM lumen. It most likely represents the processed form of the inverted M_r 34000 peptide. When the M_r 34000 peptide has inverted orientation, its potential signal sequence-like cleavage site downstream of TM12 is exposed to the RM lumen and therefore is accessible to a lumenal signal sequence cleavage enzyme (see Fig. 4, model II). The fact that the intensity of the M_r 34000 peptide is greatly decreased in the presence of RM strongly supports this possibility. This is also confirmed by the identification of a ~4 kDa peptide fragment associated with the membrane pellet (data not shown). This fragment most likely represents the transmembrane segments consisting of TM11 and TM12 of the M_r 34000 peptide which remained with membrane after the cleavage and release of the hydrophilic M_r 31000 fragment into RM lumen (see model II, Fig. 4). Complete removal of both the M_r 34000 and M_r 31000 peptides by proteinase K in the presence of Triton X-100 confirms that the digestion is complete (lane 9, Fig. 6). Similar results of both membrane insertion and orientation were obtained from another construct of truncated class III Pgp which has an additional 14 amino acids at the N-terminus (data not shown, but see Fig. 1a for the amino acid sequence). Therefore, the short amino terminus of the truncated class III Pgp was not responsible for its reduced insertion ability and more inverted orientation.

These results indicate that the M_r 34000 product of pCPGP-3C DNA has less ability to target and associate with the membrane than the peptide A product of pMPGP-2C (class II) DNA and the peptide A′ product of pCPGP-1C (class I) DNA, even though all these products have two similar TM segments. Perhaps factors in addition to the transmembrane domains are

required for efficient membrane insertion and proper orientation.

Effects of charged amino acids surrounding the hydrophobic domains on the proper membrane integration of the M_r 36000 peptide A of class II Pgp

It has been demonstrated in prokaryotic systems that the balance of positively charged residues surrounding the transmembrane domains determines the topology of the molecule and affects the efficiency of its membrane integration [25–27]. The truncated class III Pgp molecule has different membrane insertion and orientation characteristics than truncated class I and II Pgps. Sequence comparison shows that class III Pgp has a different charge distribution surrounding the last two TM segments (see Fig. 1). To investigate whether the charged residues surrounding TM11 and TM12 of truncated Pgps affect their membrane integration and orientation, we made two mutant pMPGP-2C DNA constructs (denoted as M1 and M2 respectively). The M1 mutant has Thr-52 and Glu-54 (as numbered in Fig. 1a) changed to arginine and lysine, respectively and the M2 mutant has Lys-15 and Lys-16 (as numbered in Fig. 1a) changed to asparagine and glutamine,

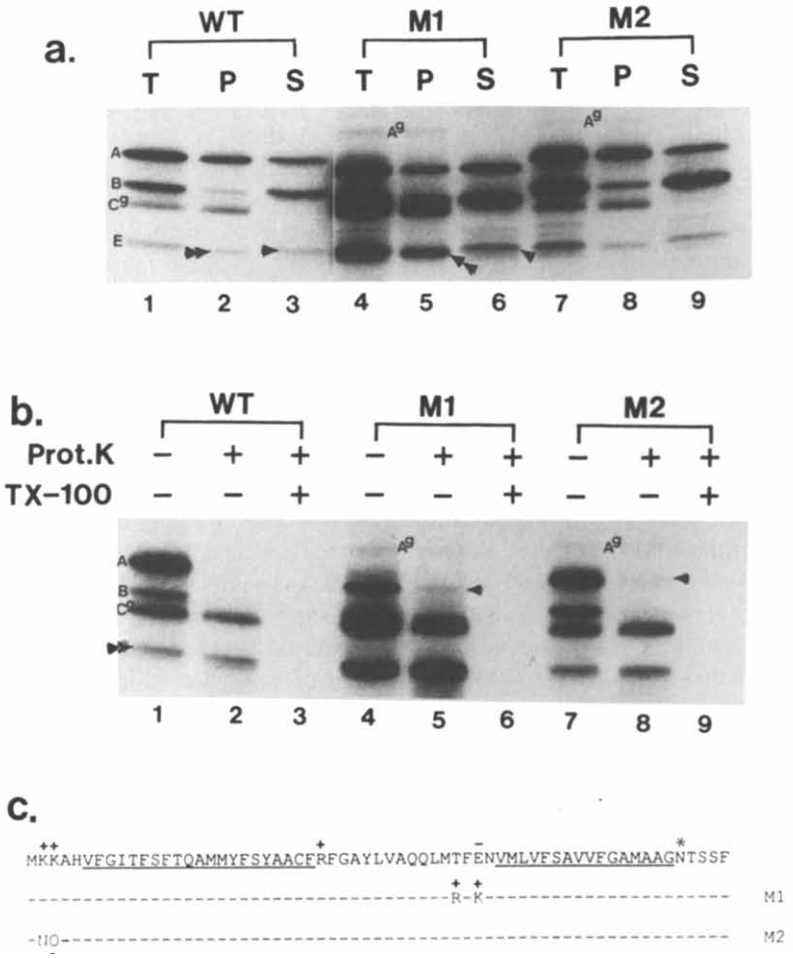

Fig. 7. (a) Membrane association of wild type and mutant M_r 36000 peptide A. Translation was carried out in rabbit reticulocyte lysate in the presence of RM with wild type (WT), or mutant (M1 and M2) pMPGP-2C transcripts. The membrane pellets (P) were separated from non-membrane fractions (S) by centrifugation and each fraction was analyzed on SDS-PAGE. About 60%, (WT, lane 2), 40% (M1, lane 6), 65% (M2, lane 8) of peptide A were membrane-associated. The calculation was accomplished by dividing the intensity (determined by Densitometer) of peptide A-associated with membrane by the total intensity of peptide A both in pellet and supernatant. Lanes 1, 4 and 7 are total translation products. It is worth noting that the addition of positive charges in the linking domain (M1) affects the mobility of the peptide A (see lane 4). (b) Membrane orientation of wild type and mutant M_r 36000 peptide A. Membrane fractions from WT, M1 and M2 translation were treated with proteinase K in the absence (lanes 2, 5 and 8) or presence (lanes 3, 6 and 9) of Triton X-100. 5–10% (M1) and 10–20% (M2) of the peptide A were resistant to proteinase K digestion (indicated by arrow head in lanes 5 and 8). On the other hand, all of peptide A of WT was sensitive to the proteinase digestion (lane 2, also see lane 7 of Fig. 2b). A band of higher molecular weight (indicated by A^g) of M1 and M2 was also resistant to proteinase digestion (lanes 5 and 8). The peptide C^g and its unglycosylated precursor of all constructs were resistant to proteinase digestion (lanes 2, 5 and 8), same observation as in Fig. 2b. The calculation was performed as in (a). (c) Sequences of the wild type and mutant mouse *mdr1* Pgp. The top line shows the wild type sequence. The M1 mutant has a Thr and a Glu residue changed to Arg and Lys respectively. The M2 mutant has two Lys residues changed to Asn and Gln residues, respectively.

respectively (see Fig. 7c). Mutant DNAs were isolated and used for in vitro translation analysis.

Fig. 7a shows the results of membrane integration of wild type (WT) and mutant class II Pgps. Differential centrifugation shows that ~ 60% of WT peptide A and ~ 65% of M2 mutant peptide A remained with the membrane pellet (lanes 2 and 8). This number goes down to 40% for the M1 mutant peptide A (lane 5). However, more peptides C^g and its unglycosylated precursor (double arrowhead, lane 5) were generated from the M1 mutant. This is probably due to processing of inverted molecules of peptide A (see discussion for Fig. 7b). Considering the increased amount of peptides C^g and its unglycosylated precursor (indicated by double arrowhead, lane 5) generated from the peptide A in M1 mutant, it is clear that membrane targeting and integration of the peptide A (the sum of peptides A with right and inverted orientations) of M1 mutant is not significantly different from WT and the M2 mutant. Therefore, mutations of charged amino acids surrounding TM11 and TM12 did not affect the membrane association of truncated Pgp molecules. The majority of peptide B is not membrane-associated and most peptide C^g is membrane vesicle-associated in all cases. Furthermore, there is also a slightly increased amount of proteinase-resistant peptide A generated from mutant DNA as shown in Fig. 7b. Proteinase K treatment of the membrane-associated translation products shows that a small fraction of the M1 and M2 mutant peptides A (indicated by arrowhead in lanes 5 and 8 of Fig. 7b) were protected from digestion, whereas none of the WT peptide A was protected (also see lane 7, Fig. 2b). This suggests that these proteinase-resistant mutant proteins have their long C-terminal ends located in the lumen of RM vesicles and therefore represent the molecules with inverted orientation. Particularly, more peptide C^g with its unglycosylated form (indicated by double arrowhead) and less peptide A was generated from M1 mutant construct as compared with the WT and M2 construct (compare lanes 1, 4, 7 and lanes 2, 5, 8 in Fig. 7b). This may be due to the increase of inverted orientation of the peptide A which will give rise the production of peptide C^g and its unglycosylated form by signal sequence cleavage (see model II in Fig. 4). This is supported by the observation that the intensity of the peptide A M1 mutant is decreased in the presence of RM (data not shown). Similar results were also observed with the truncated class III Pgp molecules (Fig. 6). Proteinase-resistant peptides of higher molecular weight (indicated by A^g in Fig. 7a and Fig. 7b) were also generated from mutant DNAs but not from WT DNAs (compare lanes 2, 5 and 8, Fig. 7b, also see Fig. 2). These peptides are membrane-associated (lanes 5 and 8, Fig. 7a). They were reduced to M_r 36000 by PNGaseF treatment (data not shown), suggesting that they are glycosylated and that the C-terminal domain with potential N-linked glycosylation site Asn-72 is located in the RM lumen. The above results show that the membrane orientation of a fraction peptide A is altered by replacing with amino acids of different charge.

Discussion

We have successfully translated truncated P-glycoproteins containing the predicted TM11 and TM12 of all three classes using a cell-free system. The truncated class I and II Pgps inserted into membranes efficiently. The ATP-binding domain and monoclonal antibody C219 epitope are oriented on the outside of RM vesicles (corresponding to an intracellular location) and presumably the peptide linking TM11 and TM12 forms an extracellular loop. This is consistent with our in vitro study using full-length molecules [15] and also in vivo studies [5]. It appears that TM11 functions as a signal sequence while TM12 functions as a stop-transfer sequence when both are present in the same nascent peptide. We conclude, therefore, that TM11 and TM12 are used to signal membrane insertion and anchorage of the truncated peptides of class I and II Pgps.

We have also compared the difference in membrane associateion and orientation between the non-MDR-associated (class III) and MDR-associated (class I and II) Pgp molecules. Our results here show that the last two TM segments of class III Pgp may have membrane orientation and insertion characteristics different from class I and II Pgps. More inverted orientation of the truncated class III Pgp was observed and they may be processed into M_r 31000 peptide by signal sequence cleavage (see model II in Fig. 4). This phenomenon was also observed with the translation study of the M1 mutant construct (Fig. 7). Although it is not known what role TM11 and TM12 play in the membrane association and orientation of the full-length molecules, it is significant that transfection of the full-length human Pgp genes into BRO human melanoma cells showed difference between membrane association of the class I and class III Pgps [8]. Only 5–10% of the class III transfected cells expressed detectable protein on the cell surface although the total amount of membrane-associated class III Pgp was similar to class I Pgp, as determined by Western blot analysis. On the other hand, virtually all class I Pgp transfected cells have Pgp molecules expressed on the cell surface. It is possible that class III Pgp cannot insert properly into membranes in these cells and therefore cannot be transported to the cell surface efficiently. Furthermore, in our previous study, the C-terminal half molecule of mouse *mdr1* Pgp (class II) has been shown to have a different topological orientation from the prediction. Recently, by expression of full-length and truncated C-terminal half molecules of human *mdr1* (class I) Pgp,

Skach et al. [35] have made a similar observation of the topological orientation of the C-terminal half molecules. Together, these results suggest that truncated molecules in an in vitro system behave similarly as a full-length molecules in vivo.

Previously, it has been shown that the charged amino acids surrounding the TM segments influence membrane orientation of both prokaryotic and eukaryotic membrane proteins [25–29]. However, the role of charged amino acids surrounding the TM regions of a polytopic membrane protein in eukaryotes is less well-understood. Sequence comparison showed that one of the regions conserved between class I and II, but not in class III is at TM11 and TM12 [6, 16]. The linking peptide between TM11 and TM12 has higher net positive charges in class III than in class I and II Pgp. In this study, we have shown that altering the charges of amino acids surrounding the TM domains can also change the membrane orientations but not membrane targeting of the truncated class II Pgp. Although it has been shown previously that charged amino acids also affect the membrane orientation of eukaryotic proteins with a single transmembrane domain [28,29], to our knowledge the current study is the first attempt to show the effects of charged amino acids on membrane orientation of an eukaryotic membrane protein that spans membrane more than once. It was postulated in prokaryotes that positively charged residues in the signal sequence interact with cytoplasmic negatively charged residues in components of the secretion apparatus [26]. Thus it appears that the "positive charge inside" rule proposed by von Heijne [30] for prokaryotes is also applicable to mammalian membrane proteins that span membrane multiple times. Recently, Simon and Blobel [31] have demonstrated the presence of protein-conducting channels for protein secretion in eukaryotic microsomes. It is tempting to speculate that in the context of our current findings positive amino acid residues surrounding the signal sequence of an eukaryotic nascent peptide interact with negative residues of the putative protein-conducting channel and thus halt the translocation of positively charged domains.

The class III Pgp apparently does not confer an MDR phenotype even though it is homologous with class I and II Pgps, which are associated with MDR. The structural basis for this functional difference may involve the net positive charge of amino acids surrounding the TM domains. Previously, it has been demonstrated that an exchange of either the N-terminal (amino acids 411–544) or C-terminal (amino acid 1123 to the C-terminus) ATP-binding domain of class I Pgp with that of class III Pgp does not affect the MDR function. In contrast, class I Pgp loses its MDR function when the TM domains with their surrounding amino acids (TM1 to TM4, TM1 to TM6, or TM7 to TM12) are replaced by the corresponding domain of class III Pgp [9]. These replacement were not restricted only to the predicted TM segments as the surrounding amino acids were also exchanged. In light of our findings, it is possible that the effect observed by Buschman and Gros [9] may be due to the exchange of TM-surrounding charged amino acids which affect the membrane insertion and orientation. It is interesting to note that there are also differences in charge distribution between MDR-associated and non-MDR-associated Pgps surrounding TM2 and TM8 [6,16].

The class III Pgp is highly expressed in some differentiated normal tissues, e.g. skeletal muscle cells where apparently the class III Pgp is membrane-associated, although its function in these tissues remains unknown [32,33]. It is tempting to speculate that in these differentiated cells, other components may be present that can accommodate the relevant charged amino acids surrounding the TM domains of the class III Pgp. Thus, the class III Pgp in these cells can properly fold and insert into the appropriate membranes for function. It was demonstrated recently that glucose transporters (GLUT's) have isoform-specific subcellular targeting [34]. While GLUT1 was found primarily on the cell surface of transfected mouse fibroblasts, GLUT4 was directed to vesicles in a perinuclear distribution and could not perform its hexose uptake function [34]. All these observations suggest that special components may be required to assist proper protein folding and trafficking. Thus, it is possible that a drug resistance phenotype or a transport function may be identified with the class III Pgp if it is expressed into cells that have such analogous accessory components.

Acknowledgements

This work is supported by the National Cancer Institute of Canada and by public service grant CA37130 from the National Institute of Health, USA to V.L. J.T.Z. is a recipient of post-doctoral fellowship from the National Cancer Institute of Canada. We would like to thank Dr. P. Gros (McGill University, Canada) for his kind gift of the mouse *mdr1* cDNA. We would also like to thank our colleagues from Ontario Cancer Institute for their critical reading of this manuscript and helpful discussions.

References

1 Deverson, E.V., Gow, I.R., Coadwell, W.J., Monaco, J.J., Butcher, G.W. and Howard, J.C. (1990) Nature 348, 738–741.
2 Trowsdale, J., Hanson, I., Mockridge, I., Beck, S., Townsend, A. and Kelly, A. (1990) Nature 348, 741–744.
3 Spies, T., Bresnahan, M., Bahram, S., Arnold, D., Blanck, D., Mellins, E., Pious, D. and DeMars, R. (1990) Nature 348, 744–747.
4 Juranka, P.F., Zastawny, R.L. and Ling, V. (1989) FASEB J. 3, 2583–2592.

5 Endicott, J.A. and Ling, V. (1989) Annu. Rev. Biochem. 58, 137–171.
6 DeVault, A. and Gros, P. (1990) Mol. Cell. Biol. 10, 1652–1663.
7 Devine, S.E., Ling, V. and Melera, P.W. Proc. Natl. Acad. Sci. USA 89, 4564–4568.
8 Shinkel, A.S., Roelofs, M.E.M. and Borst, P. (1991) Cancer Res. 51, 2628–2635.
9 Buschman, E. and Gros, P. (1991) Mol. Cell. Biol. 11, 595–603.
10 Gros, P., Dhir, R., Croop, J. and Talbot, T. (1991) Proc. Natl. Acad. Sci. USA 88, 7289–7293.
11 Greenberger, L.M., Lisanti, C.J., Silva, J.T. and Horwitz, S.B. (1991) J. Biol. Chem., 266, 20744–20751.
12 Blobel, G. (1980) Proc. Natl. Acad. Sci. USA 77, 1496–1500.
13 Audigier, Y., Friedlander, M. and Blobel, G. (1987) Proc. Natl. Acad. Sci. USA 84, 5783–5787.
14 Andrews, D. (1989) Bio Tech. 7, 960–967.
15 Zhang, J.T. and Ling, V. (1991) J. Biol. Chem. 266, 18224–18232.
16 Endicott, J.A., Sarangi, F. and Ling, V. (1991) DNA Sequence 2, 89–101.
17 Melton, D.A., Krieg, P.A., Rebagliati, M.R., Maniatis, T., Zinn, K. and Green, M.R. (1984) Nucleic Acids Res. 12, 7035–7057.
18 Howell, K.K. and Palade, G.E. (1982) J. Cell Biol. 92, 822–832.
19 Walter, P., Ibrahimi, I. and Blobel, G. (1981) J. Cell Biol. 91, 545–550.
20 Gilmore, R., Blobel, F. and Walter, P. (1982) J. Cell Biol. 95, 463–469.
21 Meyer, D. and Dobberstein, B. (1980) J. Cell Biol. 87, 498–502.
22 Georges, E., Zhang, J.T. and Ling, V. (1991) J. Cell. Physiol. 148, 479–484.
23 Moos, M., Nguyen, N.Y. and Liu, T.Y. (1988) J. Biol. Chem. 263, 6005–6008.
24 Gerlach, J.H., Endicott, J.A., Juranka, P.F., Henderson, G., Sarangi, F., Deuchars, K.L. and Ling, V. (1986) Nature 324, 485–489.
25 Boyd, D. and Beckwith, J. (1989) Proc. Natl. Acad. Sci. USA 86, 9446–9550.
26 Boyd, D. and Beckwith, J. (1990) Cell 62, 1031–1033.
27 Nilsson, I. and von Heijne, G. (1990) Cell 62, 1135–1141.
28 Beltzer, J.P., Fiedler, K., Fuher, C., Geffen, I., Handschin, C., Wessels, H.P. and Spiess, M. (1991) J. Biol. Chem. 266, 973–978.
29 Parks, G.D. and Lamb, R.A. (1991) Cell 64, 777–787.
30 von Heijne, G. (1986) EMBO J. 5, 3021–3027.
31 Simon, S.M. and Blobel, G. (1992) Cell 65, 371–380.
32 Georges, E., Bradley, G., Gariepy, J. and Ling, V. (1990) Proc. Natl. Acad. Sci. USA 87, 152–156.
33 Bradley, G., Georges, E. and Ling, V. (1990) J. Cell. Physiol. 145, 398–408.
34 Hudson, A.W., Ruiz, M. and Birnbaum, M.J. (1992) J. Cell Biol. 116, 785–797.
35 Skach, W.R., Calayag, M.C. and Lingappa, V.R. (1993) J. Biol. Chem. 268, 6903–6908.